Comparing heat mapping methodologies in the metropolitan Adelaide context

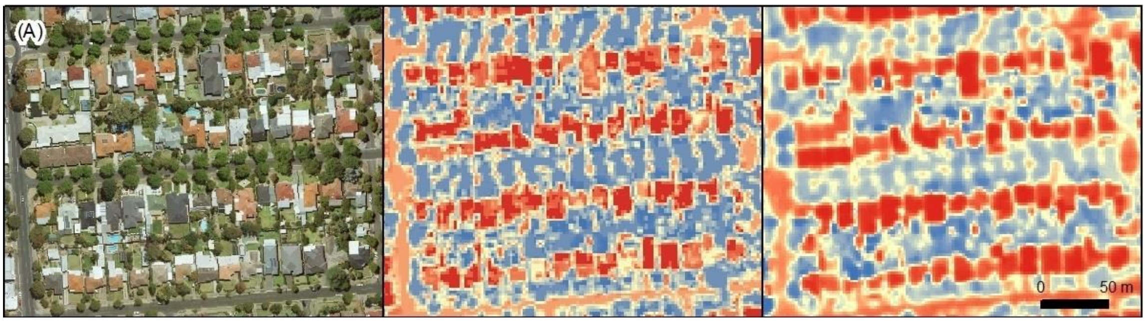

Blair Kavanagh and Zafi Bachar
Natural Resources Adelaide and Mount Lofty Ranges
February 2018

Government of South Australia
Natural Resources Adelaide and Mt Lofty Ranges

Contents

List of tables

List of figures

Acronyms

AMLR	Adelaide and Mount Lofty Ranges
ASTER	Advanced Spaceborne Thermal Emission and Reflection Radiometer
CRC for WSC	Cooperative Research Centre for Water Sensitive Cities
GIS	Geographic information systems
LST	Land surface temperature
MODIS	Moderate-resolution imaging spectroradiometer
NASA	National Aeronautics and Space Administration
NDVI	Normalised difference vegetation index
NIR	Near infrared
NRM	Natural resources management
SWIR	Short-wave infrared
TIRS	Thermal infrared sensor
USGS	United States Geological Survey
WSC	Water sensitive cities
WSUD	Water sensitive urban design

Acknowledgements

We wish to acknowledge and thank the following partners who contributed data and expertise to this project:

- CRC for Water Sensitive Cities
- Resilient South councils (comprising of the Cities of Holdfast Bay, Marion, Mitcham and Onkaparinga)
- Adapt West councils (comprising of the Cities of Charles Sturt, Port Adelaide Enfield and West Torrens)
- City of Playford
- City of Unley
- Seed Consulting Services
- EnDev Geographic
- Airborne Research Australia.

1 Executive summary

In response to a changing climate, extreme heat days and heatwaves in Adelaide are expected to increase. As a result, the city's metropolitan councils have become increasingly interested in heat mapping to gain insights into local heat distribution, including urban heat island locations. While air temperature measurements provide a more accurate indication of human thermal comfort, land surface temperature (LST) is often used as an economical proxy. Over the past few years, several LST mapping projects have been undertaken within metropolitan Adelaide, each using one of the following three methods:

- airborne thermal imagery
- satellite thermal imagery (using Landsat data)
- LST modelling using the Water Sensitive Cities (WSC) Modelling Toolkit's Extreme Heat Module.

Through a desktop review involving four case study areas across the metropolitan region (focussing only on daytime heat mapping), this project has:

- evaluated the intrinsic strengths and weaknesses of each method
- evaluated the accuracy of the WSC Modelling Toolkit's Extreme Heat Module against airborne and satellite heat mapping
- made some general recommendations regarding which methodology may be the most advisable under given circumstances.

The comparison of the LST modelling with both the airborne thermal imagery and the Landsat thermal imagery revealed that while each method returns different temperature values, which cannot be used to predict another method's resulting values, all methods provide a relative indication of urban heat distribution. A summary comparison of these methods is provided in Table A.

This study can advise councils who are planning to undertake heat mapping of the pros and cons of each method and assist in decision making on which is the appropriate methodology to use in a given circumstance.

Table A. Summarised comparison of heat mapping methodologies

	LST modelling	Airborne	Landsat satellite
Cost	• $1,000s • Includes time taken for a suitably trained staff member to complete modelling • Price will vary depending on the extent of the project area	• $10,000s • Includes acquisition, processing and analysis of the imagery by a specialist operator • Price will vary depending on the extent of the project area • Will be more cost effective if larger areas are acquired at the same time and if multiple partners are engaged	• $1,000s • Includes post-processing and analysis of the imagery by a specialist operator • Raw dataset is free to download • Price is unlikely to vary considerably for extents within the Adelaide metropolitan region
Appropriate scale	• Streetscape • Reserve • Suburb • Small municipality	• Single municipality • Multiple municipalities	• Large municipality • Multiple municipalities • Whole city
Spatial resolution	• Project defined, however 5-10 m is recommended	• Project defined, however typically 2-5 m	• 100 m (resampled to 30 m in delivered data product)
Temporal resolution	• Not representative of a particular day • Somewhat dependent on the currency of the classification (i.e. imagery which the classification is based on) • Ability to modify land cover classes to explore the potential future impact of implementing WSUD and green infrastructure features	• Flight day and time is project defined • Potential for daytime and night-time capture • Only one point in time	• 16 day overpass schedule • 11 am capture (approximately) • Archive of thermal imagery from 1982 onwards from various Landsat satellites (Landsat 4, 5, 7 and 8)
Data accessibility	• WSC Modelling Toolkit is available through the CRC for WSC • Outputs can be viewed using GIS software	• Requires a specialist operator to acquire and process the imagery • Outputs can be viewed using GIS software	• Raw dataset is downloadable from the USGS (via Earth Explorer or GloVis websites) • Requires a specialist operator to process the imagery • Outputs can be viewed using GIS software
Secondary products	• LSTs after implementing WSUD and green infrastructure features	• Products from any additional cameras/sensors carried during the flight, such as aerial photography, NIR, albedo and multi-spectral data	• Products derived from Landsat's visible, NIR and SWIR bands, such as true colour image, false colour image and NDVI
Key limitations	• Reliant on a land cover classification • Does not detect variation within single land cover class • Single temperature is applied to all roofs	• Most expensive mapping method • Requires appropriate post-processing to get accurate values • Requires ideal capture condition	• Coarsest spatial resolution • Satellite overpass is unlikely to correspond to an extreme heat event • Not good at detecting areas with mixed land covers

2 Background

With extreme heat days and heatwaves expected to increase in response to a changing climate, governments are becoming increasingly aware of their responsibility to reduce the impact of urban heat. While high air temperatures have the greatest impact on human thermal comfort, measuring localised air temperatures over large areas can be costly and difficult, therefore land surface temperature (LST) is often used as a surrogate. LST mapping provides insight into heat distribution, including the location of urban heat islands, and can be done at various scales, such as a city scale, council scale or finer scales such as streets or reserves.

In the past few years, Adelaide metropolitan councils have become increasingly interested in the use of LST mapping. As a result, several heat mapping projects have been undertaken using different methodologies and technical specification to inform the management of urban heat within councils, and ultimately increase the resilience of communities to extreme heat events (see Table 1). Objectives of these projects include:

- Identifying patterns of heat across the municipality
- Identifying urban heat islands
- Identifying public spaces most susceptible to urban heat
- Identifying where urban heat is likely to impact particularly vulnerable members of the community
- Investigating how urban heat is influenced by the design and distribution of landscape features
- Prioritising areas for water sensitive urban design (WSUD) and green infrastructure features
- Modelling the potential microclimatic benefits of implementing WSUD and green infrastructure features.

The results of these projects will inform decision making in many areas of urban planning and public policy, as well as the prioritisation of human thermal comfort related interventions.

The Adelaide and Mount Lofty Ranges (AMLR) Natural Resources Management (NRM) Board also has an interest in urban heat mapping projects. The board has identified urban heat as a persistent and ongoing issue within metropolitan Adelaide and is committed to supporting the mitigation of the impact of urban heat by facilitating the transition to water sensitive communities.

The board undertakes work through the regional NRM Plan action LM-22 '*Encourage the increased adoption of water sensitive urban design through capacity building programs and demonstration sites*', as well as more broadly through action CC-2 '*Support the development of locally relevant climate change adaptation responses*' (AMLR NRM Board, 2016).

With the increasing interest in urban heat mapping, one of the key decisions faced by all project leaders is which heat mapping methodology to apply. Project requirements, budgets and organisational preferences tend to vary, and project leaders will always select a heat mapping methodology to suit their specific organisational circumstances. To date, the following methods have been applied to various heat mapping projects in Adelaide (see Table 1):

- airborne thermal imagery
- satellite thermal imagery (specifically Landsat)
- LST modelling using the Water Sensitive Cities (WSC) Modelling Toolkit's Extreme Heat Module.

However the differences between these methods are not always clear and the resultant implications of the method choice for heat mapping projects may not be well understood. This project seeks to address these issues by reviewing and comparing these three heat mapping methodologies. The specific objectives of this project are to:

- evaluate the intrinsic strengths and weaknesses of each method
- evaluate the accuracy of the WSC Modelling Toolkit's Extreme Heat Module against airborne and satellite heat mapping
- make some general recommendations regarding which methodology may be the most appropriate under which circumstances.

These objectives will be achieved through a desktop review involving four case study areas across the metropolitan region. While some heat mapping methodologies allow for the capture of night-time temperatures, this project will focus only on daytime heat mapping.

The remainder of the report is structured as follows:

- Chapter 3 provides a theoretical overview of each of the three heat mapping methods, as well as the strengths and weaknesses of each.
- Chapter 4 details the methods and results of the desktop study to compare heat mapping methods.
- Chapter 5 summarises the findings for each heat mapping method and provides recommendations for their use and application.

Table 1: Summary of metropolitan Adelaide heat mapping projects undertaken to date

Project	Council/s	Organisation delivering the work	Method	Date of capture	Time of capture	Maximum daytime temperature	Spatial resolution	Spatial extent	Reference
Resilient South Urban Heat Mapping	City of Holdfast Bay City of Marion City of Mitcham City of Onkaparinga	Arbor Carbon	Airborne	22 February 2016	11:25 am – 3:30 pm	39.5 °C	2 m	Multiple municipalities (285 km^2)	Arbor Carbon, 2016
Western Adelaide Urban Heat Mapping	City of Charles Sturt City of Port Adelaide Enfield City of West Torrens	Seed Consulting Services Airborne Research Australia EnDev Geographic	Airborne	9 February 2017	Day: 11 am – 4 pm Night: 11 pm – 3 am (10 February)	39.2 °C (overnight minimum 25.2 °C)	2 m	Multiple municipalities (186 km^2)	Seed Consulting Services, 2017b
City of Playford Thermal Mapping Analysis	City of Playford	Seed Consulting Services EnDev Geographic	Satellite (Landsat 8)	7 January 2016 8 February 2016	11:05 am	30.9 °C (January) 29.5 °C (February)	100 m resampled to 30 m	Single municipality (344 km^2)	Seed Consulting Services, 2017a
City of Unley Urban Microclimate Benefits	City of Unley	CRC for WSC	LST modelling	N/A	N/A	N/A	10 m	Single municipality (14 km^2) and street (27 ha)	CRC for WSC, 2016
Microclimate Modelling for Norman Reserve, St Mary's	City of Mitcham	Natural Resources AMLR	LST modelling	N/A	N/A	N/A	5 m	Reserve (8.7 ha)	Natural Resources AMLR, 2017b
Microclimate Modelling for Gray Street, Adelaide	City of Adelaide	Natural Resources AMLR	LST modelling	N/A	N/A	N/A	5 m	Street (0.6 ha)	Natural Resources AMLR, 2017a

3 Overview of heat mapping methods

While each of the heat mapping methods reviewed in this study has its own inherent strengths and weaknesses, the following limitations are common to all three:

- The mapping captures LSTs as a surrogate for air temperatures, since the former typically demonstrates similar patterns to the latter (Coutts and Harris, 2013).
- The mapping represents the landscape as a two-dimensional surface and does not account for the thermal properties of three-dimensional surfaces, such as green walls, which are known to have a cooling effect.

The following sections provide further details regarding the strengths and weaknesses of each method.

3.1 Airborne thermal imagery

Airborne thermal imagery is often viewed as the premium heat mapping method, mostly due to its high spatial resolution and the broad applicability of the data it generates.

The capture of airborne thermal imagery requires the mounting of a thermal imaging camera onto a specialist remote sensing aircraft which is then flown over the study area. The spatial resolution, which is controlled by the height of the aircraft during the flight, typically ranges from 2 to 5 m but can be captured as low as 0.5 m if project requirements dictate.

Flight timing is also flexible, enabling both daytime and night-time imagery capture, however consideration needs to be given to the timing of the flight, particularly daytime flights. Importantly, flights should be timed to coincide with an extreme heat day (preferably following another or multiple extreme heat days) as well as clear (cloud and haze free) flying conditions. The flight should also target solar noon so as to minimise the effects of shading and to detect the maximum surface temperatures for the day (Harris and Coutts 2011, Coutts and Harris 2013).

Airborne thermal imagery requires appropriate post-processing in order to accurately represent LSTs in the final product. Ideally, post-processing should include a correction for emissivity, which will vary considerably across the urban landscape due to each surface's unique ability to emit radiation at a given temperature. For example, vegetation has higher emissivity than hard surfaces, and roofs have highly variable emissivity dependent on the colour and material used in their construction (summarised in Coutts and Harris 2013). In high resolution airborne thermal imagery, where distinct surfaces are identifiable within a single pixel, an appropriate emissivity correction should be applied each surface rather than assume equal emissivity.

Applying an emissivity correction is however often difficult, since it relies on an accurate land surface classification. As a result, emissivity corrections are often not applied to airborne thermal imagery, or equal emissivity is assumed. In these instances, it is likely that surface temperatures are underestimated, particularly for roofs, which have highly variable emissivity. In either case, a specialist operator is required to acquire, process and analyse the imagery.

Key strengths

- The spatial resolution of the imagery can be selected according to project needs, including the option of high resolution products up to approximately 0.5 m.
- The flight path can be defined based on project needs.
- The flight time can be chosen to target suitable conditions during both daytime and night-time.
- Secondary products, such as aerial photography, can be acquired at the same time as acquiring the thermal product.

Key weaknesses

- Airborne thermal imagery requires appropriate post-processing in order to achieve an accurate product.
- A specialist operator must be engaged to acquire, process and analyse the imagery.
- The imagery is typically captured over a period of a few hours over a day, therefore can be subject to changing conditions through the duration of the flight.
- The window of opportunity for imagery capture is typically fairly limited, and much time can be spent waiting for ideal flying and capture conditions.
- Due to its high cost and very specific weather condition requirements, this method does not lend itself to frequent repeat captures, thus limiting the opportunity for temporal comparisons.

3.2 Landsat satellite thermal imagery

Several remote sensing satellites, such as MODIS, Landsat and ASTER, capture thermal data at varying spatial and temporal resolutions. This project focuses on Landsat Project satellites, which are operated jointly by the USGS and NASA and have been used in several urban heat mapping projects locally and interstate (for example Phan and Coutts 2014; Seed Consulting Services 2017a).

The latest satellite in the Landsat series is Landsat 8, launched in 2013[1]. In addition to capturing visible, near infrared (NIR) and short-wave infrared bands (SWIR), Landsat 8 contains a thermal infrared sensor (TIRS) which captures two thermal bands – band 10 which has a wavelength of 10.60-11.19 µm and band 11 which has a wavelength 11.50-12.51 µm. These thermal bands are captured at a spatial resolution of 100 m, but are resampled to 30 m for the delivered data product.

Each Landsat 8 scene covers an area approximately 170 km by 185 km, and the entire Adelaide metropolitan region is covered within one scene. Repeat capture of each scene occurs every 16 days at approximately 11 am Adelaide time.

---

[1] Prior to 2013, band 6 in Landsat 7's Enhanced Thematic Mapper Plus (ETM+) sensor captured thermal signatures with a wavelength of 10.40-12.50 µm at a spatial resolution of 60 m (resampled to 30 m). The Landsat 7 satellite was launched in 1999, but suffered a scan line corrector failure in 2003. Imagery collected after this failure is missing approximately 22% of the pixels within any given scene.
Landsat 4 (in operation from 1982 to 1993) and Landsat 5 (in operation from 1984 to 2013) also captured thermal data with their Thematic Mapper (TM) sensors. Both satellites captured thermal signatures within band 6 with a wavelength of 10.40-12.50 µm at a spatial resolution of 120 m (resampled to 30 m).

The long archive of Landsat imagery (thermal bands have been captured since Landsat 4 was launched in 1982), its spatial resolution, and the free access to its data make Landsat a suitable satellite for assessing the distribution of urban heat across large areas, such as entire metropolitan areas or large municipalities.

The Landsat data products for band 10 and 11 do not contain temperature values, but rather pixel values which must undergo initial post-processing (through the application of a series of formulas) in order to derive LSTs. Further post-processing should also correct for emissivity, using a normalised difference vegetation index (NDVI) and the NIR band (as outlined in Martin *et al.* 2015). However, several projects assume uniform emissivity by applying a single emissivity value to the entire scene when converting the thermal bands to LSTs (see appendix 37 in Arbor Carbon 2016; U.S. Geological Survey 2016).

Key strengths

- The entire metropolitan Adelaide area is captured in one scene.
- Raw Landsat datasets are available from the USGS free of charge.
- The Landsat archive contains thermal imagery from 1982 onwards which can be used to assess temporal changes in urban heat.
- Landsat captures bands in the visible, NIR and SWIR portions of the spectrum, which can be used to generate secondary products such as NDVI.

Key weaknesses

- Extreme heat events are unlikely to coincide with Landsat's 16 day overpass schedule.
- The satellite overpass occurs at approximately 11 am which is unlikely to coincide with the maximum daily temperatures.
- Satellite imagery requires cloud free conditions in order to be useful for heat mapping purposes.
- The Landsat satellite only ever captures daytime imagery.
- Landsat 8's thermal band is captured at a spatial resolution of 100 m (then resampled to 30 m) and while this resolution is considered relatively high for a satellite product, it is much coarser than that provided through airborne imagery.
- Due to the satellite imagery's relatively coarse spatial resolution, each pixel is influenced by several underlying land covers, which are then effectively averaged within the pixel.

3.3 Land surface temperature modelling

The final method evaluated in this project is LST modelling as performed by the Extreme Heat Module of the WSC Modelling Toolkit[2], which was developed by the CRC for WSC in 2016 and revised in 2017. The module was designed as a conceptual tool to not only understand the distribution of heat within the landscape, but also to assess the potential microclimate benefits of modifying the land surface cover by implementing WSUD and green infrastructure features (CRC for WSC, 2017).

[2] The WSC Modelling Toolkit also currently contains the Stream Erosion and Minor Flooding module, Stream Hydrology and Water Quality module and Treatment and Harvesting module.

The Extreme Heat Module models LSTs based on a land cover classification. A user-defined grid is applied over the classification and the module calculates the LSTs based on the land cover classes within each grid cell. The temperatures that underpin the model are based on measurements from surface temperature sensors collected in the City of Port Phillip (in inner Melbourne) on 26 February 2012, when maximum air temperature reached 37 °C (Coutts and Harris 2013, and see Figure 1).

While the module only contains surface temperature measurements for the seven basic land cover classes of 'tree', 'water', 'dry grass', 'irrigated grass', 'roof', 'road' and 'concrete', it enables LST modelling of common WSUD and green infrastructure features by classifying:

- ponds, basins and wetlands as 'water'
- swales as 'dry grass'
- biofilters, infiltration systems, green roofs and green walls as 'irrigated grass'
- porous pavements as 'road'.

Within the module any land cover class can be substituted for another to quantify the potential cooling or warming effect caused through land cover change.

The WSC Modelling Toolkit is currently available to CRC for WSC members or parties who have undergone relevant training, however the CRC for WSC intends to make it more widely available and is in the process of establishing an Extreme Heat Module user group.

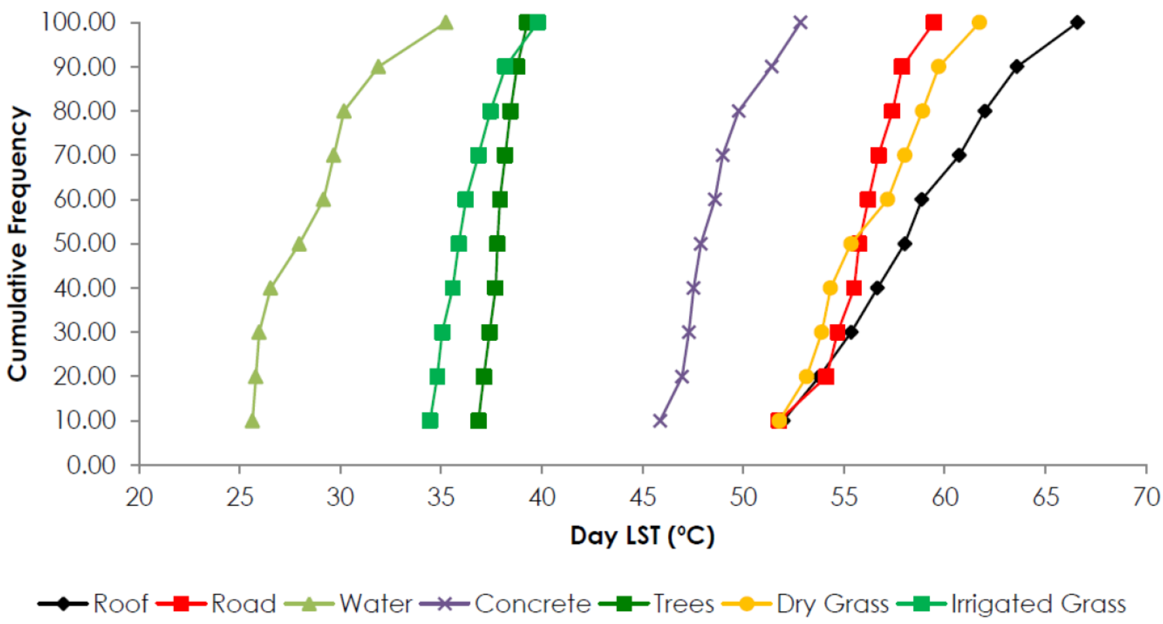

Figure 1: LSTs measured on 26 February 2012 in the City of Port Phillip underpinning the Extreme Heat Module's thermal signatures for each land cover class (Source: CRC for WSC, 2017).

Key strengths

- The Extreme Heat Module models (and quantifies) the potential local cooling benefits of implementing WSUD and green infrastructure features within the landscape, as well as modelling LSTs.

- The module does not require any specialist skills other than a working knowledge of geographic information systems (GIS) in order to create a land cover classification.
- Modelling can be undertaken at any time and does not rely on ideal flying conditions or a satellite overpass.
- The spatial resolution can be modified to match project requirements.

Key weaknesses

- The modelling is reliant on a land cover classification dataset as its sole input, and is therefore sensitive to classification inaccuracies (as further discussed in Section 4.2).
- The modelling does not account for LST variation within a single land cover class.
- Since all LSTs are modelled, the results do not represent any particular point in time.

4 Heat mapping methodology comparison and analysis

This study compared heat mapping methodologies in four 1 km^2 case study areas (as denoted in Figure 2) – one in the City of Mitcham, one in the City of Unley and two in the City of Playford (in Elizabeth and in Andrews Farm). Case studies were undertaken in areas already mapped using one of the three methods and were selected to ensure a mixture of land cover classes.

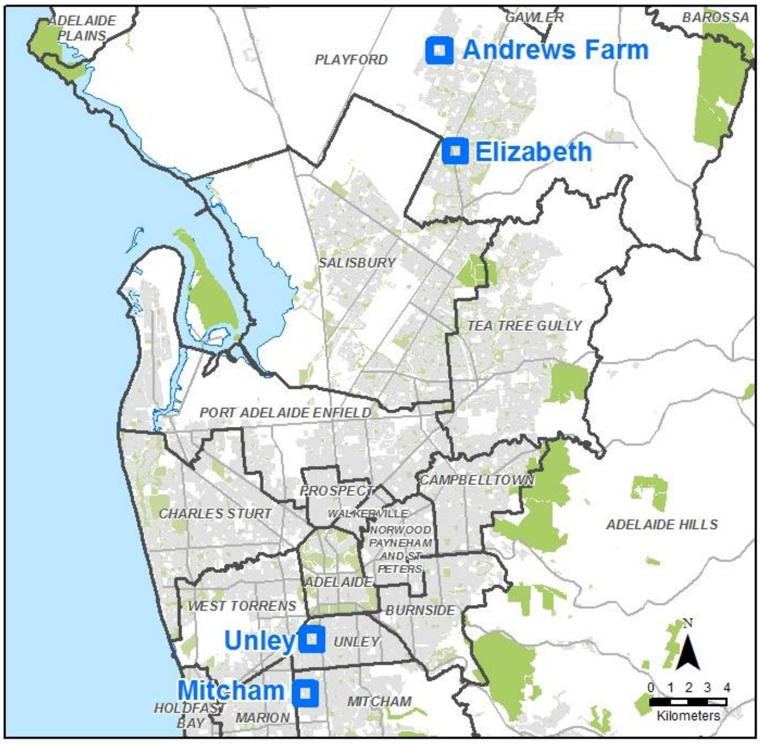

Figure 2: Location of case study areas (in blue) within metropolitan Adelaide

Two case studies compared airborne thermal imagery with LST modelling (Mitcham and Unley) and two compared Landsat thermal imagery with LST modelling (Elizabeth and Andrews Farm; see Table 2).

Table 2: Heat mapping datasets used for the comparison within each case study area

Case study area	Heat mapping datasets
Mitcham	1) Airborne thermal imagery from the Resilient South Urban Heat Mapping Project 2) LST modelling generated specifically for the purpose of this project
Unley	1) Airborne thermal imagery from the Western Adelaide Urban Heat Mapping Project^ 2) LST modelling from the City of Unley Microclimate Benefits Project
Elizabeth	1) Landsat thermal imagery from the City of Playford Thermal Mapping Analysis Project 2) LST modelling generated specifically for the purpose of this project
Andrews Farm	1) Landsat thermal imagery from the City of Playford Thermal Mapping Analysis Project 2) LST modelling generated specifically for the purpose of this project

^ This dataset was a by-product of the Western Adelaide Urban Heat Mapping Project and was processed specifically for this project

4.1 Case study areas

The Mitcham case study area covers the suburbs of Melrose Park, Clarence Gardens, Cumberland Park, Daw Park and Colonel Light Gardens (see Figure 3A). It predominantly contains residential land uses, though some commercial areas are found in the west of the case study area along South Road. Edwardstown Primary School lies in the centre of the case study area and Bailey Reserve lies in the north.

Figure 3: Aerial photography and landmarks within the Mitcham (A), Unley (B), Elizabeth (C) and Andrews Farm (D) case study areas

The Unley case study area covers the suburbs of Forestville, Goodwood, Millswood, Wayville and Black Forest (see Figure 3B). It predominantly contains residential land uses, though some commercial areas are found in the north along Leader Street and the east along Goodwood Road. The Unley Swimming Pool lies in the centre of the case study area, Goodwood Primary

School lies in the east and Goodwood Oval lies in the south. The case study area is bisected by the Belair/Seaford train line from north to south and the Glenelg tram line from east to west.

The Elizabeth case study area in the City of Playford covers the suburbs of Elizabeth, Elizabeth East and Elizabeth Park (see Figure 3C). It contains a mixture of residential and commercial land uses (including Elizabeth City Centre Shopping Centre), as well as Fremont Park in the north east and several reserves along Main North Road, which bisects the case study area from north to south. Elizabeth East Primary School lies in the south east.

The Andrews Farm case study area in the City of Playford covers the suburb of Andrews Farm and Smithfield Plains (see Figure 3D). It contains a mixture of residential areas and reserves, including Andrews Park, Kooranowa Reserve and Stebonheath Park, which contains the Stebonheath Park Wetlands. St Columba College lies in the centre of the case study area.

4.2 Land cover classification

Land cover classifications were generated for the Mitcham, Elizabeth and Andrews Farm case study areas prior to undertaking the LST modelling (as per Table 2). These classifications were generated in ArcMap by applying a supervised classification to a 7.5 cm resolution aerial photograph from February 2016. The land cover classes followed the classes and codes provided in the module user guide (CRC for WSC 2017; Table *3*). Following the initial classification, the dataset was resampled to 60 cm and filtered to remove excess noise in the classification. As a final step to improving the classification, a vector road layer was imprinted onto the classification in all areas except where roads were covered by trees (as detailed in CRC for WSC 2016). A similar process was carried out to imprint the Stebonheath Park Wetlands into the Andrews Farm classification.

Table 3: Land cover classes and codes required for the Extreme Heat Module

Land cover class	Code
Tree	1
Water	2
Pond and basin*	3
Dry grass	5
Irrigated grass	7
Roof^	12
Road	13
Concrete	15

* *Only used in the Elizabeth and Andrews Farm case study areas*
^ *Initially classified into four classes based on the colour of the roof material (white, grey, red and green) and then merged into a single class*

Each land cover classification clearly identifies the distribution of land surfaces within the case study area (see Figure 4) and can be used to highlight the similarities and differences between land surfaces in each of the case study areas (Figure 5). For example, while the dominant land cover classes in all case study areas are trees and roofs, Andrews Farm contains the lowest proportion of tree canopy and instead contains higher proportions of concrete and ponds. Mitcham and Unley, which contain the highest proportions of roofs also contain the lowest proportion of dry grass – especially Unley.

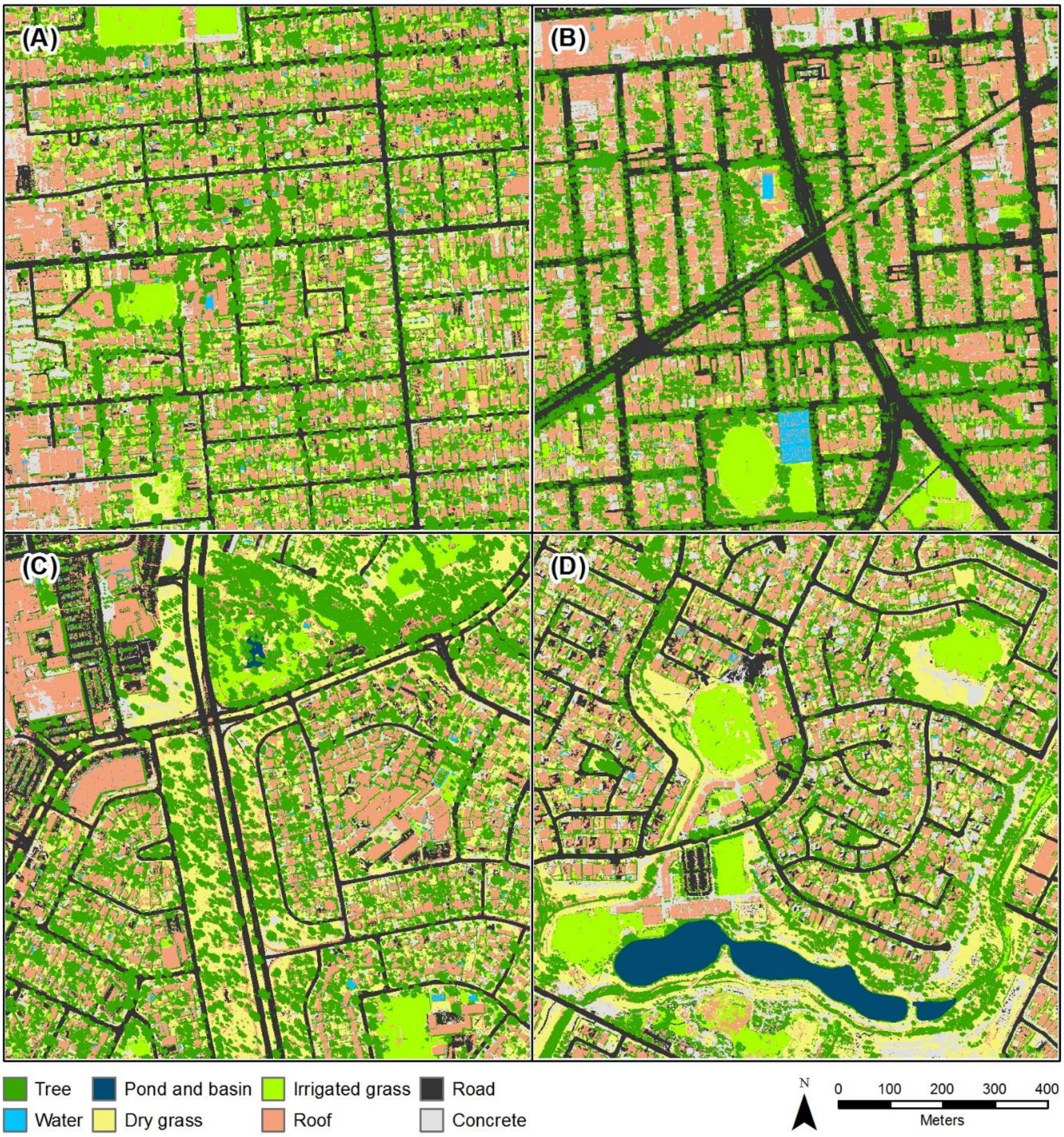

Figure 4: Land cover classifications within the Mitcham (A), Unley (B), Elizabeth (C) and Andrews Farm (D) case study areas

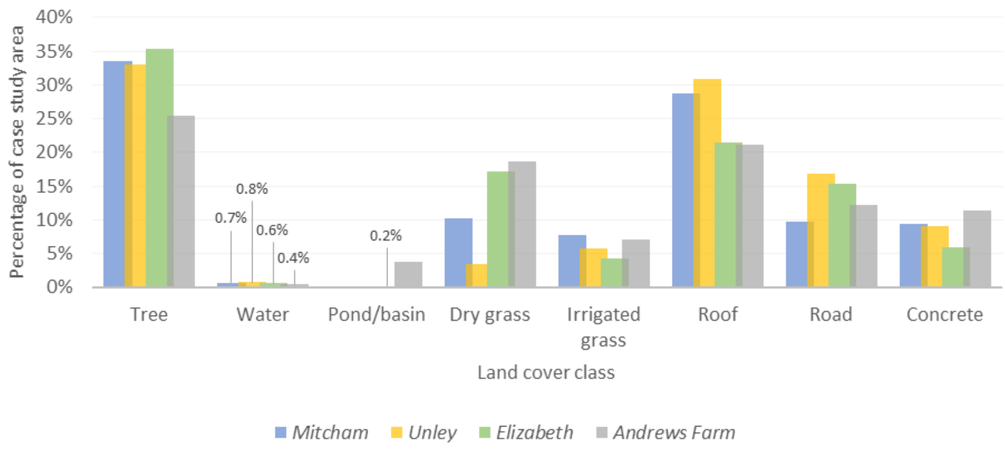

Figure 5: Proportion of land cover classes within each case study area

Each classification underwent an accuracy assessment to detect how well the aerial photography is represented by the land surface classification. A total of 80 randomly generated locations were assessed per land cover class per case study area. The accuracy of the classifications ranged from 66% to 69%, with the exception of the Unley classification which scored 53% (see Appendix A: accuracy assessments).

Despite time and effort being spent in refining training sites to improve the classification, the accuracy assessments highlighted that achieving a high accuracy land cover classification is difficult, due to the following key factors:

- The aerial photography's spectral resolution – the aerial photography used for the classification only contains bands in the visible part of the spectrum (red, green and blue). As a result all pixels are classified based on their colour alone, increasing the potential for misclassification. For example, misclassification occurred when:
    - Landscape features from two different classes had a similar colour (e.g. roads and grey roofs, tree and irrigated grass, dry grass and concrete).
    - The colour of landscape features differs from the conventional expectation (e.g. hard surface sports courts painted blue or green). The water class was particularly susceptible to over-classification since all blue features (including blue cars, blue roofs and blue painted hard surfaces) were classified as water.
- The aerial photography's spatial resolution – the aerial photography's very fine pixel size (7.5 cm) creates 'noise', which was reduced (but not completely eliminated) by resampling the classification to 60 cm and then applying a 'majority filter' to reduce small classification errors.
- The variety of roof surfaces and colours – the variety of roof surfaces and colours in the metropolitan setting makes consistent roof classification particularly difficult to achieve. The classification of roofs was based on four colours (white, grey, red and green),

however roofs which did not fall into these categories were misclassified (e.g. light brown roofs were misclassified as dry grass).

- Objects masking the 'true' land cover – misclassifications occur when objects such as cars, bins and children's play equipment cover the underlying land surfaces (such as asphalt, concrete or grass).
- Shadows – while the aerial photography is captured in the middle of the day to reduce shadowing, any shadows which still persist in the image may result in misclassification.
- The spatial extent of the classification – the larger the area, the more difficult it is to achieve a consistently accurate classification. While the other case studies were classified within 1x1 km areas, the Unley case study area's classification was derived from a much larger exercise covering the whole of the Unley municipality, and was therefore the least accurate.

4.3 Land surface temperature modelling

Each classification was used as an input to the Extreme Heat Module. A 2 m cell size was applied to the Mitcham and Unley case study areas, while a 30 m cell size was applied to the two Playford case study areas, in order to ensure the cell size was consistent with the airborne and Landsat heat mapping datasets respectively. Because the module generates LSTs using a cell size greater than that of the classification, the impact of misclassification and noise within the classification is minimised.

LSTs were generated using the 80th percentile distribution, which is consistent with the module user guide and other LST modelling projects (CRC for WSC 2017, Natural Resources AMLR 2017a and 2017b). Compared to the other options, this distribution generates the highest LSTs and is most consistent with an extreme heat day.

Stratified random sampling was applied to each case study area (200 random points per land cover class) to enable a direct comparison of temperatures between the LST modelling and either the airborne thermal imagery or the Landsat thermal imagery (as per Table 2). The temperatures were then analysed and graphed to assess how closely each dataset compared to the other.

4.4 Comparison of land surface temperature modelling with airborne thermal imagery

A visual overview of the heat mapping for the Mitcham and Unley case study areas, showing both LST modelling and airborne thermal imagery, is provided in Figure 6 and Figure 7.

Modelled LST values are significantly higher than those captured in the airborne thermal imagery, both across the whole case study area and for individual land cover classes[3] (all p-values < 0.0001[4]; see Figure 8 and Figure 9). The only exception is the water class in the Unley case study area which returns higher temperature values in the airborne thermal imagery as

---

[3] While not presented here, the results of land surface temperature modelling using the 20th and 50th percentile distributions were also significantly warmer than both the airborne thermal imagery, though the relative differences were smaller.

[4] A p-value less than 0.05 is considered statistically significant.

compared to the modelled data (Figure 9; p-value < 0.0001), a result strongly influenced by the misclassification of hard surface tennis courts as water.

Despite the differences in the resulting absolute temperatures, land cover classes assumed warmer in the LST modelling (dry grass, roofs, roads and concrete) are also shown as warmer in the airborne thermal imagery. The same is true of those land cover classes that tend to be cooler (trees, water and irrigated grass), with the exception of the Unley water category.

However when plotted directly against each other, the airborne mapping values do not clearly correlate to the modelled values (Figure 10), meaning temperature values from one dataset cannot be used to accurately predict the values in the other. Similarly individual land cover classes show no clear correlation between the methods (see Figure 18 and Figure 19 in Appendix B: correlations by land cover class).

To determine whether the strength of correlation was impacted by the accuracy of the land cover classification, the correlation analysis was repeated for the Mitcham case study area using only correctly classified points. Any resulting increased correlation was negligible, and in the case of some land cover classes the correlation actually worsened slightly, indicating that improved land cover classification accuracy does not strengthen that correlation.

The differences between the modelled results and the airborne thermal imagery are most likely caused by the Extreme Heat Module's simplified representation of the variety of LSTs across a landscape. By applying a standardised temperature to each land cover class, the modelling fails to account for the natural variation in thermal signatures within each class, which is apparent in the airborne thermal imagery. The differences may also be caused by the data underpinning the model, which being solely reliant on 14 surface temperature sensors (Coutts and Harris 2013), may not represent a large enough sample size to accurately predict the temperatures for each land cover class. This limitation is particularly relevant for highly variable land covers, such as roofs.

Other key insights emerging from a visual comparison of the two resulting mapping products at various locations are:

- The two methods often produce comparable results in residential areas and in tree lined streets (Figure 11A).
- As all roofs are assigned the same temperature in the LST modelling, some of them return very high modelled temperature values as compared to the airborne thermal imagery[5] – particularly white roofs, which are commonly recognised as being cooler than darker roofs (Figure 11B and Figure 11D).
- Easily visible hotspots in the airborne thermal imagery can be absent from the LST modelling if certain land covers had been misclassified (Figure 11C).
- Provided sufficient colour variation between dry and irrigated grass, the LST modelling can detect variability within the heat signature of reserves similar to that identified in the airborne thermal imagery (Figure 11B).

[5] Without an appropriate emissivity correction, roof values are likely to be underestimated in the airborne thermal imagery.

- Where the land cover classification consists of large areas of a single class (for example irrigated grass), the LST modelling applies a single temperature value across that entire area and will not detect any variability within it. In contrast, the airborne thermal imagery can detect subtle variation even within the same land cover, such as with areas of grass which are more heavily irrigated than others (Figure 11E).
- The LST modelling applies a slightly cooler temperature value to irrigated grass than to trees, while in the airborne thermal imagery some trees appear cooler than areas of irrigated grass (Figure 11E).
- When correctly classified, water stands out as being the coolest features in both the LST modelling and the airborne thermal imagery (Figure 11A and Figure 11C).
- Gross land cover misclassifications can result in significant thermal signature misrepresentation in LST modelling. For example, the misclassification of blue concrete as water produces a much lower modelled LST relative to the airborne thermal imagery (Figure 11E).
- A mismatch between the land cover classification's spatial resolution and the Extreme Heat Module's grid cell size can result in excess noise in the modelled heat map. For example, the Unley case study area applied a 2 m modelling grid cell over a 1 m resolution classification (Figure 11C and Figure 11E), resulting in more noise in the LST modelling than in the Mitcham case study area, where a 2 m modelling grid was used with a 0.6 m resolution classification (Figure 11A, Figure 11B and Figure 11D).

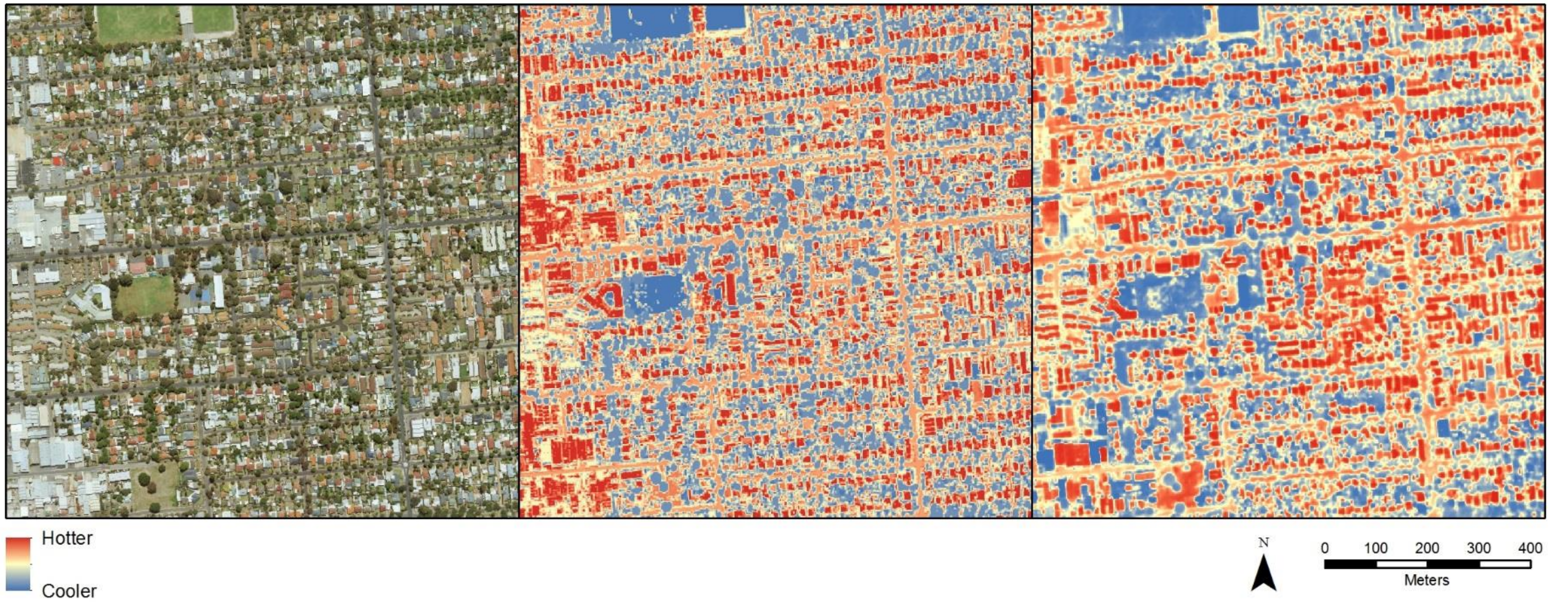

Figure 6: Mitcham case study area showing aerial photography (left) alongside heat mapping from LST modelling (centre) and airborne thermal imagery (right)

Figure 7: Unley case study area showing aerial photography (left) alongside heat mapping from LST modelling (centre) and airborne thermal imagery (right)

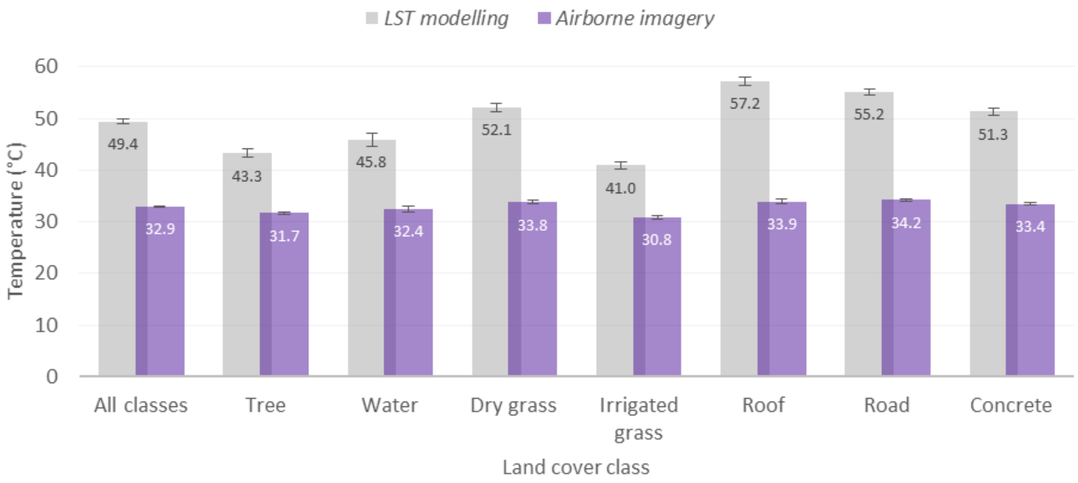

Figure 8: Comparison of mean LSTs within the Mitcham case study area.
LST modelling and airborne thermal imagery means are shown for all land cover classes combined, as well as each individual class. Error bars show 95% confidence intervals.

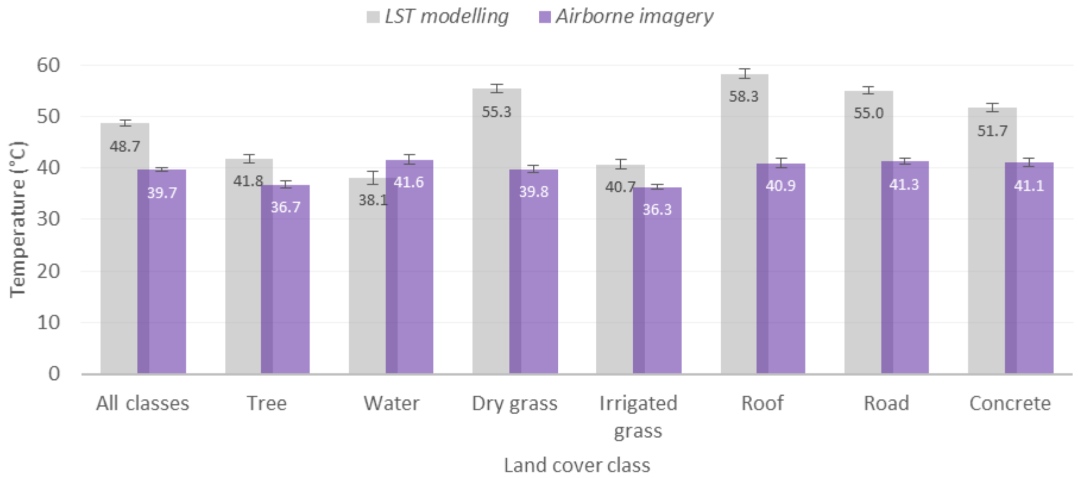

Figure 9: Comparison of mean LSTs within the Unley case study area.
LST modelling and airborne thermal imagery means are shown for all land cover classes combined, as well as each individual class. Error bars show 95% confidence intervals.

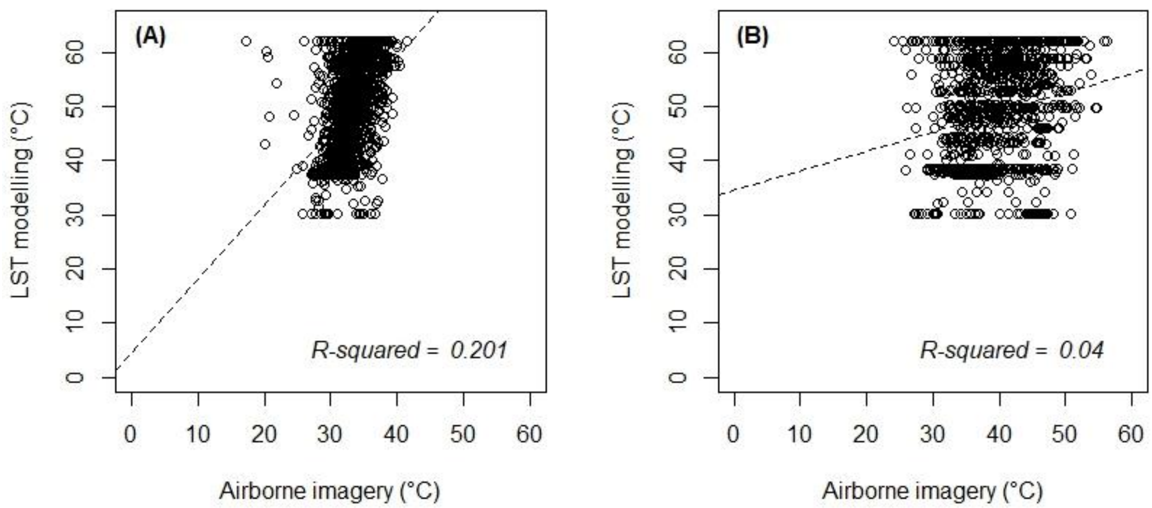

Figure 10: Correlation between airborne thermal imagery and LST modelling for Mitcham (A) and Unley (B).

Strength of the correlation is shown as an r-squared value (which can range from 0-1).

Figure 11: Examples from the Mitcham and Unley case study areas showing aerial photography (left) alongside heat mapping from LST modelling (centre) and airborne thermal imagery (right)

4.5 Comparison of land surface temperature modelling with Landsat satellite thermal imagery

A visual overview of the heat mapping for the Elizabeth and Andrews Farm case study areas, showing both the LST modelling and Landsat thermal imagery, is provided in Figure 12 and Figure 13.

As in the case of the airborne thermal imagery, modelled LST values are significantly warmer than those captured in the Landsat thermal imagery[6], both across the whole case study area and for individual land cover classes without exception (all p-values < 0.0001; Figure 14 and Figure 15). While this is consistent with the results of the airborne thermal imagery comparison, it is also likely due to the Landsat thermal imagery not representing an extreme heat day nor the hottest part of the day.

The thermal mapping (both LST mapping and Landsat) in the Elizabeth and Andrews Farm case study areas show a far smaller temperature range between difference land cover classes when compared to Mitcham and Unley (Figure 14 and Figure 15). This effect is particularly evident in the Landsat thermal imagery, where there is only a 1.4 °C difference between the warmest and coolest land cover class for the Elizabeth case study area and a 2.8 °C for the Andrews Farm case study area. This difference is likely due to the larger cell size in these case study areas, with each pixel influenced by many underlying land covers which are then effectively averaged. The result is a more homogenous heat mapping dataset when compared to the 2 m datasets.

There was no clear correlation when the Landsat mapping values were plotted directly against the extreme heat values in the Elizabeth case study area, and only a weak correlation in the Andrews Farm case study area (Figure 16), meaning temperature values from one dataset cannot be used to accurately predict the values in the other. There are also no consistent trends when individual land cover classes are considered (see Figure 20 and Figure 21 in Appendix B: correlations by land cover class).

Reasons for these quantitative differences are likely similar to the factors identified in Section 4.4 with regard to the LST modelling. The differences are further compounded by the Landsat temperatures not being truly representative of an extreme heat day (in contrast to the LST modelling) as well as the spatial resolution of the Landsat thermal imagery which essentially averages temperatures in areas of mixed land covers.

The following are other key insights emerging from a visual comparison of the two resulting mapping products at various locations:

- Large reserves are depicted as cool-spots in both the LST modelling and the Landsat thermal imagery (Figure 17A).
- Smaller reserves and treed areas can be detected as cool-spots within the 30 m LST modelling and to a lesser extent in the Landsat thermal imagery (Figure 17B).

[6] While not presented here, the results of land surface temperature modelling using the 20th and 50th percentile distributions were also significantly warmer than both the Landsat thermal imagery, though the relative differences were smaller.

- Narrow linear features which are below the spatial resolution of the Landsat thermal bands, such as rows of trees or linear waterbodies, are not detected well within the Landsat thermal imagery, but are clearly evident in the LST modelling (Figure 17C and Figure 17D).
- Large white roofs appear as noticeable cool-spots in the Landsat thermal imagery, but appear much hotter in the LST modelling (Figure 17E). As was found in the airborne thermal imagery, this is due to the modelling applying a single LST to all roofs, regardless of colour or material.
- Generally speaking, the Landsat thermal imagery provides a much more generalised result compared to the LST modelling with an equivalent pixel size, especially in areas with mixed land covers (all examples within Figure 17).

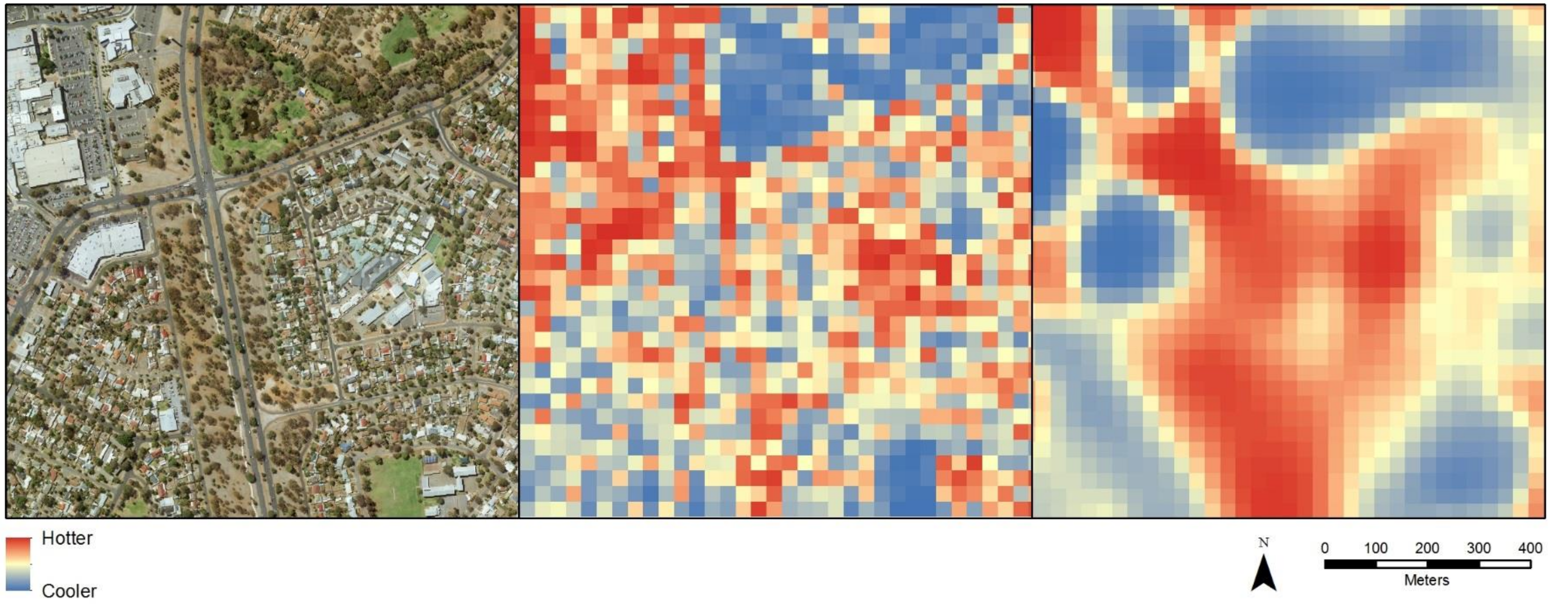

Figure 12: Elizabeth case study area showing aerial photography (left) alongside heat mapping from LST modelling (centre) and Landsat thermal imagery (right)

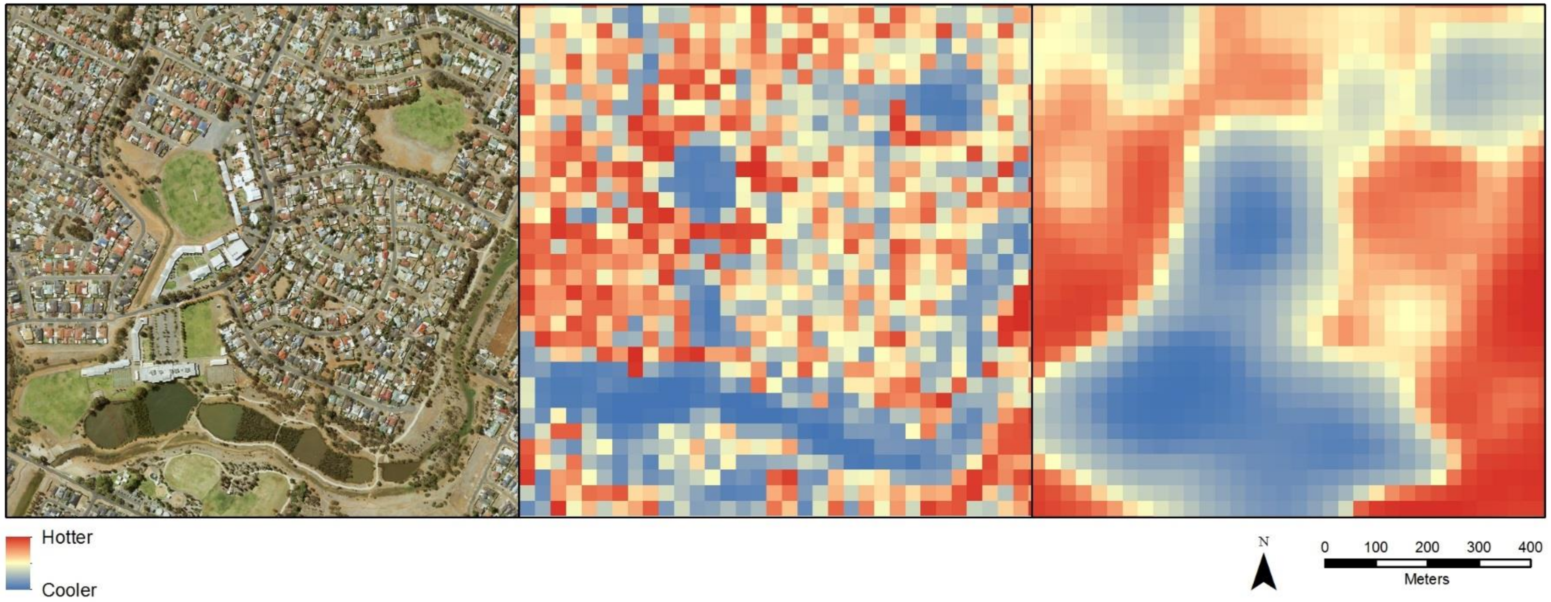

Figure 13: Andrews Farm case study area showing aerial photography (left) alongside heat mapping from LST modelling (centre) and Landsat thermal imagery (right)

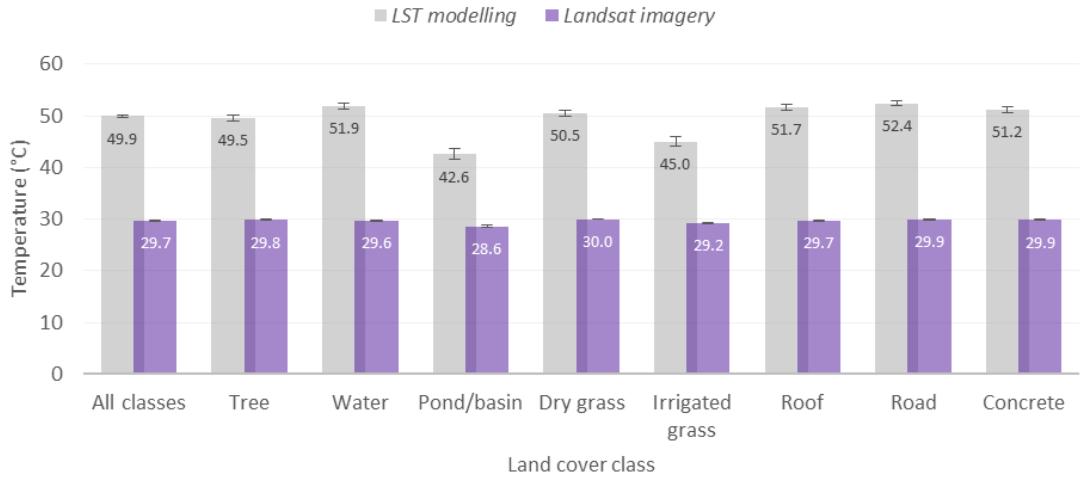

Figure 14: Comparison of mean LSTs within the Elizabeth case study area.
LST modelling and Landsat thermal imagery means are shown for all land cover classes combined, as well as each individual class. Error bars show 95% confidence intervals.

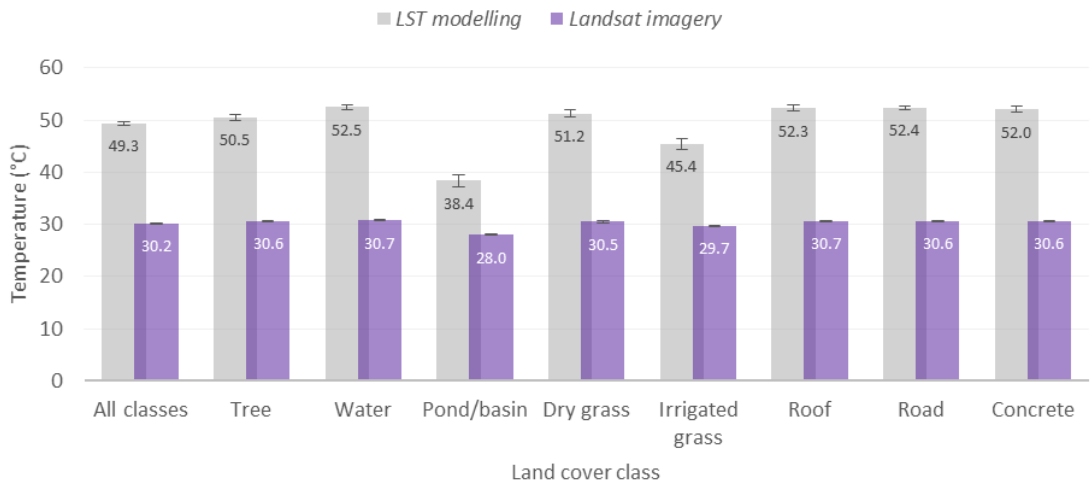

Figure 15: Comparison of mean LSTs within the Andrews Farm case study area.
LST modelling and Landsat thermal imagery means are shown for all land cover classes combined, as well as each individual class. Error bars show 95% confidence intervals.

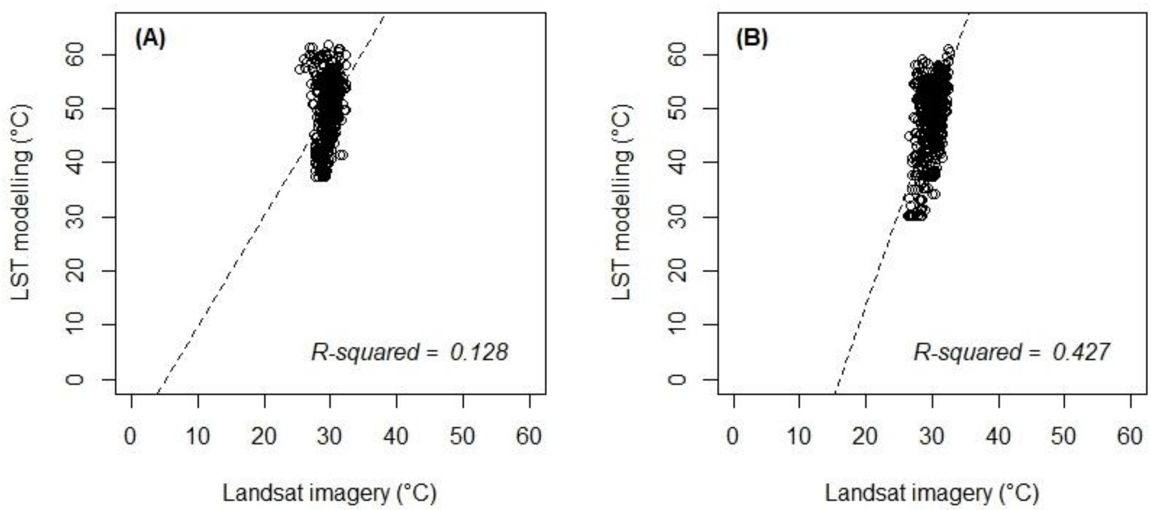

Figure 16: Correlation between Landsat thermal imagery and LST modelling for Elizabeth (A) and Andrews Farm (B).

Strength of the correlation is shown as an r-squared value (which can range from 0-1).

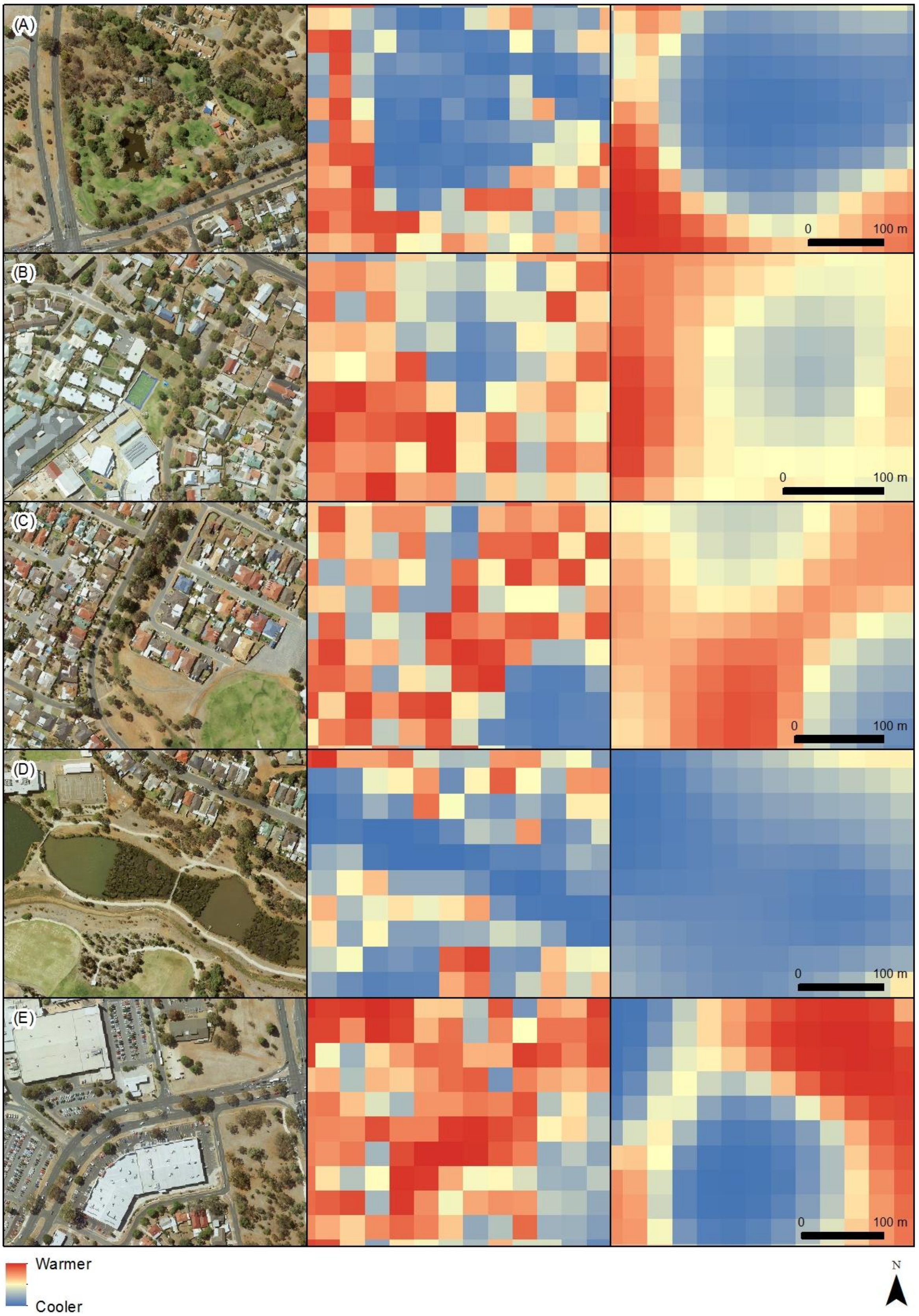

Figure 17: Examples from the Elizabeth and Andrews Farm case study areas showing aerial photography (left) alongside heat mapping from LST modelling (centre) and Landsat thermal imagery (right)

5 Summary and recommendations

The comparison of the LST modelling with both the airborne thermal imagery and the Landsat thermal imagery revealed that while each method returns different temperature values, which cannot be used to predict another method's resulting values, all methods provide a relative indication of urban heat distribution. That said, each method has its limitations and should be used with these limitations in mind.

Importantly, the comparison highlighted two key strategic questions, the answers to which would facilitate the selection of the most suitable heat mapping method, namely:

1. What is the scale and extent of the project?
2. What are the final product's intended uses?

In reference to these two key questions, key recommendations and considerations for using each method are discussed below, and a summary of each method is provided in Table 4.

5.1 Land surface temperature modelling

LST modelling is most suitable for use at finer spatial scales, mostly owing to the difficulty in achieving an accurate land cover classification as the project extent increases. LST modelling is therefore recommended for streetscapes and reserve scale project areas, and only ever for larger areas (such as small suburbs) if an accurate land cover classification can be guaranteed.

At this scale, LST modelling lends itself well to the following applications:

- Understanding the distribution of LSTs over a small urban area of particular interest.
- Visualising and quantifying the potential microclimatic benefits of implementing WSUD and green infrastructure features.

As mentioned in Section 4.2, an accurate land cover classification is important since the modelling is solely reliant on that classification to generate its LST outputs. This project generated the land cover classifications by applying a supervised classification to an aerial photograph, however classification accuracy could be improved through the following strategies:

- Undertaking manual corrections to account for gross errors in the classification. For example, in the Unley case study area, a manual correction could have been applied to reclassify the blue tennis courts as concrete rather than water. This approach is much more practical when working with small rather than large project areas, as recommended above.
- Incorporating NIR data into the supervised classification. If this additional band is available, it would improve the classification of the various vegetation land cover classes.
- Incorporating land use data or other commercially available data products into the classification. For example, the new 2 m resolution Geoscape product features relevant

land cover classes[7] and could be used to inform the land cover classification, though it too comes with its own inherent limitations.

Another important consideration when undertaking LST modelling is the choice of grid cell size. The modelling grid cell size should first and foremost be appropriate relative to the land cover classification's cell size. Based on the observations in the Unley and Mitcham case study areas, the modelling grid cell size should be at least 3 to 4 times greater than the classification cell size in order to reduce any noise in the classification. Secondly, if WSUD and green infrastructure features are being modelled, the grid cell size should be appropriate for accurately representing these features. As a general rule, a grid cell size of 5-10 m is appropriate for most urban heat mapping projects.

5.2 Airborne thermal imagery

Airborne thermal imagery is most suited to mapping urban heat over single or multiple municipalities, and is appropriate for many applications such as:

- understanding the distribution of LSTs across municipalities
- identifying urban heat islands and hot-spots
- comparing the average temperatures across suburbs and developments
- identifying public spaces most susceptible to heat
- prioritising areas for the implementation of WSUD and green infrastructure features
- investigating the heat signatures of different surfaces and materials
- informing some key planning and urban design elements of developments and public spaces.

While airborne thermal imagery is a high quality product, it is also the most expensive of the three methods, typically costing tens of thousands of dollars to acquire, process and analyse (although reducing the spatial resolution of the final product does reduce the overall cost). It is therefore most cost effective in multi-stakeholder projects mapping large areas.

While not considered in this study, night-time heat data is currently only available through airborne thermal imagery[8].

It is important to acknowledge, however, that airborne thermal imagery requires appropriate post-processing in order to obtain accurate LST values. Without such processing, the temperatures of certain surfaces (particularly roofs), are likely to be underestimated.

5.3 Landsat satellite thermal imagery

Landsat thermal imagery has the coarsest spatial resolution of the three heat mapping methods investigated in this study. It is therefore only appropriate to apply at coarse scales, such as a whole metropolitan region, multiple municipalities or a single large municipality (as was done for the City of Playford).

[7] Geoscape contains the following land cover classes: bare earth, road and path, grass, trees, unspecified vegetation, built up areas, water, buildings, cloud, shadow and swimming pool.

[8] At the time of writing this report, the CRC for WSC was in the process of incorporating night-time LST data into a future version of the Extreme Heat Module.

Landsat thermal imagery is captured at a resolution coarser than is typically useful in detailed planning decision making. It is however appropriate in cases where high resolution thermal imagery is not required, for example when wishing to identify:

- general patterns in the distribution of LSTs across an entire city or multiple municipalities
- urban heat islands at a coarse scale
- temporal changes in LST across an entire city or across multiple municipalities.

While Landsat represents larger areas with distinct land covers quite well, it is not well suited to representing urban heat in areas with mixed land covers since temperature values are averaged within each pixel. Unfortunately, there is little that can be done to overcome this limitation – it is simply incumbent on the user to select a product suitable for the scale and predicted application of their heat mapping project.

Table 4: Summarised comparison of heat mapping methodologies

	LST modelling	Airborne	Landsat satellite
Cost	• $1,000s • Includes time taken for a suitably trained staff member to complete modelling • Price will vary depending on the extent of the project area	• $10,000s • Includes acquisition, processing and analysis of the imagery by a specialist operator • Price will vary depending on the extent of the project area • Will be more cost effective if larger areas are acquired at the same time and if multiple partners are engaged	• $1,000s • Includes post-processing and analysis of the imagery by a specialist operator • Raw dataset is free to download • Price is unlikely to vary considerably for extents within the Adelaide metropolitan region
Appropriate scale	• Streetscape • Reserve • Suburb • Small municipality	• Single municipality • Multiple municipalities	• Large municipality • Multiple municipalities • Whole city
Spatial resolution	• Project defined, however 5-10 m is recommended	• Project defined, however typically 2-5 m	• 100 m (resampled to 30 m in delivered data product)
Temporal resolution	• Not representative of a particular day • Somewhat dependent on the currency of the classification (i.e. imagery which the classification is based on) • Ability to modify land cover classes to explore the potential future impact of implementing WSUD and green infrastructure features	• Flight day and time is project defined • Potential for daytime and night-time capture • Only one point in time	• 16 day overpass schedule • 11 am capture (approximately) • Archive of thermal imagery from 1982 onwards from various Landsat satellites (Landsat 4, 5, 7 and 8)
Data accessibility	• WSC Modelling Toolkit is available through the CRC for WSC • Outputs can be viewed using GIS software	• Requires a specialist operator to acquire and process the imagery • Outputs can be viewed using GIS software	• Raw dataset is downloadable from the USGS (via Earth Explorer or GloVis websites) • Requires a specialist operator to process the imagery • Outputs can be viewed using GIS software
Secondary products	• LSTs after implementing WSUD and green infrastructure features	• Products from any additional cameras/sensors carried during the flight, such as aerial photography, NIR, albedo and multi-spectral data	• Products derived from Landsat's visible, NIR and SWIR bands, such as true colour image, false colour image and NDVI
Key limitations	• Reliant on a land cover classification • Does not detect variation within single land cover class • Single temperature is applied to all roofs	• Most expensive mapping method • Requires appropriate post-processing to get accurate values • Requires ideal capture condition	• Coarsest spatial resolution • Satellite overpass is unlikely to correspond to an extreme heat event • Not good at detecting areas with mixed land covers

6 References

Adelaide and Mount Lofty Ranges Natural Resources Management Board 2016, *Adelaide and Mount Lofty Ranges Natural Resources Management Plan, Volume 2, Business and Operational Plan, 2016-17 to 2018-19*, http://www.naturalresources.sa.gov.au/files/sharedassets/adelaide_and_mt_lofty_ranges/corporate/amlr-business-operational-plan-2016-17.pdf

Arbor Carbon 2016, *Airborne Thermal Imagery and Analysis 2016, Resilient South, Report No. 16-04 prepared for Resilient South 22 May 2016*, http://onkaparingacity.com/public/download.jsp?id=78421&page=/onka/living_here/sustainable_onkaparinga/climate_change/resilient_south/project_outputs.jsp.

Coutts A and Harris R 2013, *Technical Report: A multi-scale assessment of urban heating in Melbourne during an extreme heat event: policy approaches for adaptation*.

CRC for Water Sensitive Cities 2016, *Supporting the strategic planning of City of Unley (SA) towards a water sensitive city by quantifying the urban microclimate benefits using the Water Sensitive Cities Modelling Toolkit*.

CRC for Water Sensitive Cities 2017, *Water Sensitive Cities Modelling Toolkit User Manual*.

Harris R and Coutts A 2011, *Technical Report: Airborne Thermal Remote Sensing for Analysis of the Urban Heat Island*.

Martin P, Baudouin Y, Gachon P 2015, An alternative method to characterize the surface urban heat island, *International Journal of Biometeorology*, 59:849-861.

Natural Resources Adelaide and Mount Lofty Ranges 2017a, *Microclimate Modelling for Gray Street, Adelaide, Quantifying and visualising the surface cooling benefits of proposed tree planting along a key CBD pedestrian corridor*.

Natural Resources Adelaide and Mount Lofty Ranges 2017b, *Microclimate Modelling for Norman Reserve, St Mary's, Quantifying and visualising the surface cooling benefits of Water Sensitive Urban Design features*.

Phan T, Coutts A 2014, *Land surface temperature derived from Landsat 8 Operational Land Imager (OLI) and Thermal Infrared Sensor (TIRS) technical report for Marrickville City Council, New South Wales*.

Seed Consulting Services 2017a, *Thermal mapping analysis for the City of Playford Project Report 18 July 2017*.

Seed Consulting Services 2017b, *Western Adelaide Urban Heat Mapping Project Report July 2017*.

U.S. Geological Survey 2016, *Landsat 8 (L8) Data Users Handbook, Version 2.0*, https://landsat.usgs.gov/sites/default/files/documents/Landsat8DataUsersHandbook.pdf.

7 Appendices

7.1 Appendix A: accuracy assessments

Table 5: Accuracy assessment of the Mitcham land cover classification

		Ground reference data							TOTAL	Consumer's accuracy	Commission error
		Tree (1)	Water (2)	Dry grass (5)	Irrigated grass (7)	Roof (12)	Road (13)	Concrete (15)			
Classified data	Tree (1)	54		3	7	6	2	8	*80*	68%	33%
	Water (2)	1	25	1	2	36	4	11	*80*	31%	69%
	Dry grass (5)	1		41	3	14	1	20	*80*	51%	49%
	Irrigated grass (7)	3			75	1		1	*80*	94%	6%
	Roof (12)			4	1	62	5	8	*80*	78%	23%
	Road (13)				1	10	64	5	*80*	80%	20%
	Concrete (15)			4		23	3	50	*80*	63%	38%
TOTAL		*59*	*25*	*53*	*89*	*152*	*79*	*103*	*560*		
Producer's accuracy		92%	100%	77%	84%	41%	81%	49%			
Omission error		8%	0%	23%	16%	59%	19%	51%			

Overall classification accuracy	66%
Kappa statistic	0.61

Table 6: Accuracy assessment of the Unley land cover classification

		Ground reference data							TOTAL	Consumer's accuracy	Commission error
		Tree (1)	Water (2)	Dry grass (5)	Irrigated grass (7)	Roof (12)	Road (13)	Concrete (15)			
Classified data	Tree (1)	51	1	1	6	4	12	5	*80*	64%	36%
	Water (2)		18		2	9		51	*80*	23%	78%
	Dry grass (5)	6		26	7	24	1	16	*80*	33%	68%
	Irrigated grass (7)	12		1	58	4		5	*80*	73%	28%
	Roof (12)	4		2	7	58		9	*80*	73%	28%
	Road (13)	8			1	2	61	8	*80*	76%	24%
	Concrete (15)	5		2	1	41	6	25	*80*	31%	69%
TOTAL		*86*	*19*	*32*	*82*	*142*	*80*	*119*	*560*		
Producer's accuracy		59%	95%	81%	71%	41%	76%	21%			
Omission error		41%	5%	19%	29%	59%	24%	79%			

Overall classification accuracy	53%
Kappa statistic	0.45

Table 7: Accuracy assessment of the Elizabeth land cover classification

		Ground reference data								TOTAL	Consumer's accuracy	Commission error
		Tree (1)	Water (2)	Pond/basin (3)	Dry grass (5)	Irrigated grass (7)	Roof (12)	Road (13)	Concrete (15)			
Classified data	Tree (1)	55		1	5	1	2	4	12	*80*	69%	31%
	Water (2)		4				51	19	6	*80*	5%	95%
	Pond/basin (3)	19		56	1	1			3	*80*	70%	30%
	Dry grass (5)				69		4		7	*80*	86%	14%
	Irrigated grass (7)	5				73			2	*80*	91%	9%
	Roof (12)	2			6		51	10	11	*80*	64%	36%
	Road (13)	3			6		1	63	7	*80*	79%	21%
	Concrete (15)				18		11	1	50	*80*	63%	38%
TOTAL		*84*	*4*	*57*	*105*	*75*	*120*	*97*	*98*	*640*		
Producer's accuracy		65%	100%	98%	66%	97%	43%	65%	51%			
Omission error		35%	0%	2%	34%	3%	58%	35%	49%			

Overall classification accuracy	66%
Kappa statistic	0.61

Table 8: Accuracy assessment of the Andrews Farm land cover classification

		Ground reference data								TOTAL	Consumer's accuracy	Commission error
		Tree (1)	Water (2)	Pond/basin (3)	Dry grass (5)	Irrigated grass (7)	Roof (12)	Road (13)	Concrete (15)			
Classified data	Tree (1)	60			5	3	1	1	10	*80*	75%	25%
	Water (2)		25		3	3	34		15	*80*	31%	69%
	Pond/basin (3)			79		1				*80*	99%	1%
	Dry grass (5)	1			61	7	6		5	*80*	76%	24%
	Irrigated grass (7)	5				73			2	*80*	91%	9%
	Roof (12)	2			16	1	58		3	*80*	73%	28%
	Road (13)				5		14	50	11	*80*	63%	38%
	Concrete (15)				19	1	19	4	37	*80*	46%	54%
TOTAL		*68*	*25*	*79*	*109*	*89*	*132*	*55*	*83*	*640*		
Producer's accuracy		88%	100%	100%	56%	82%	44%	91%	45%			
Omission error		12%	0%	0%	44%	18%	56%	9%	55%			

Overall classification accuracy	69%
Kappa statistic	0.65

7.2 Appendix B: correlations by land cover class

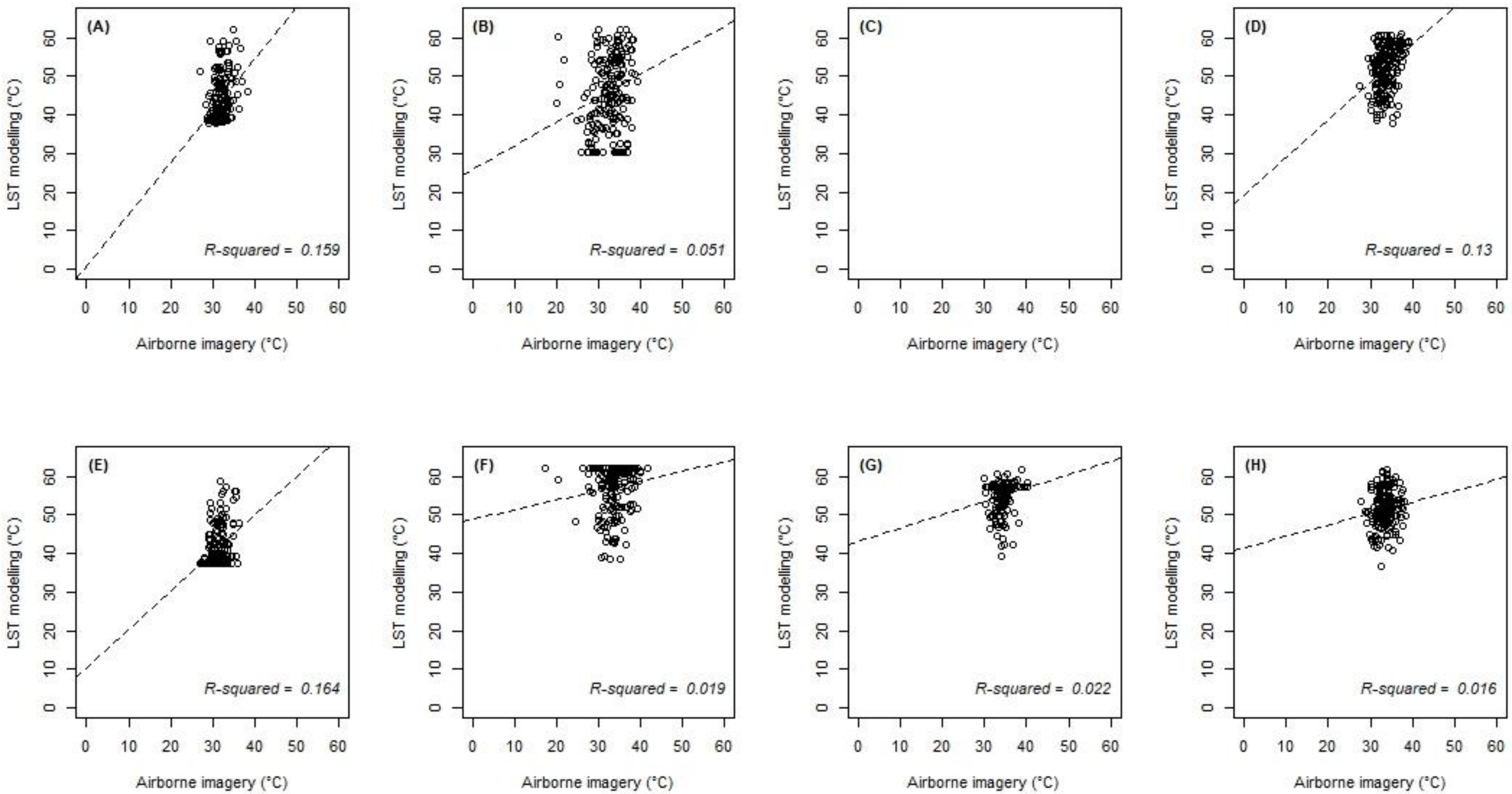

Figure 18: Correlation between airborne thermal imagery and LST modelling for each land cover class within the Mitcham case study area. Strength of the correlation is shown as the r-squared value within each graph. (A) Tree; (B) Water; (C) Pond/basin; (D) Dry grass; (E) Irrigated grass; (F) Roof; (G) Road; (H) Concrete.

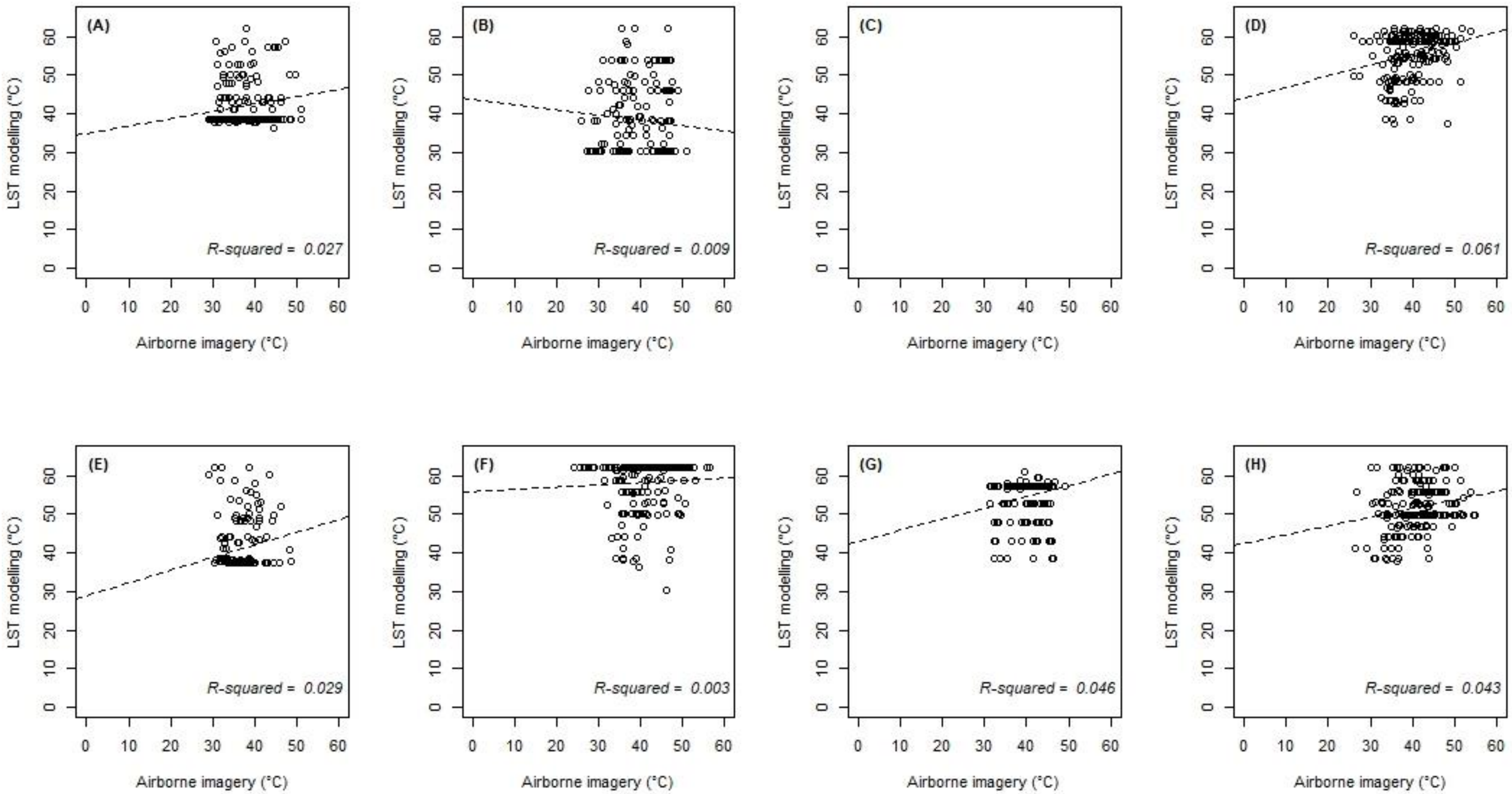

Figure 19: Correlation between airborne thermal imagery and LST modelling for each land cover class within the Unley case study area.
Strength of the correlation is shown as the r-squared value within each graph. (A) Tree; (B) Water; (C) Pond/basin; (D) Dry grass; (E) Irrigated grass; (F) Roof; (G) Road; (H) Concrete.

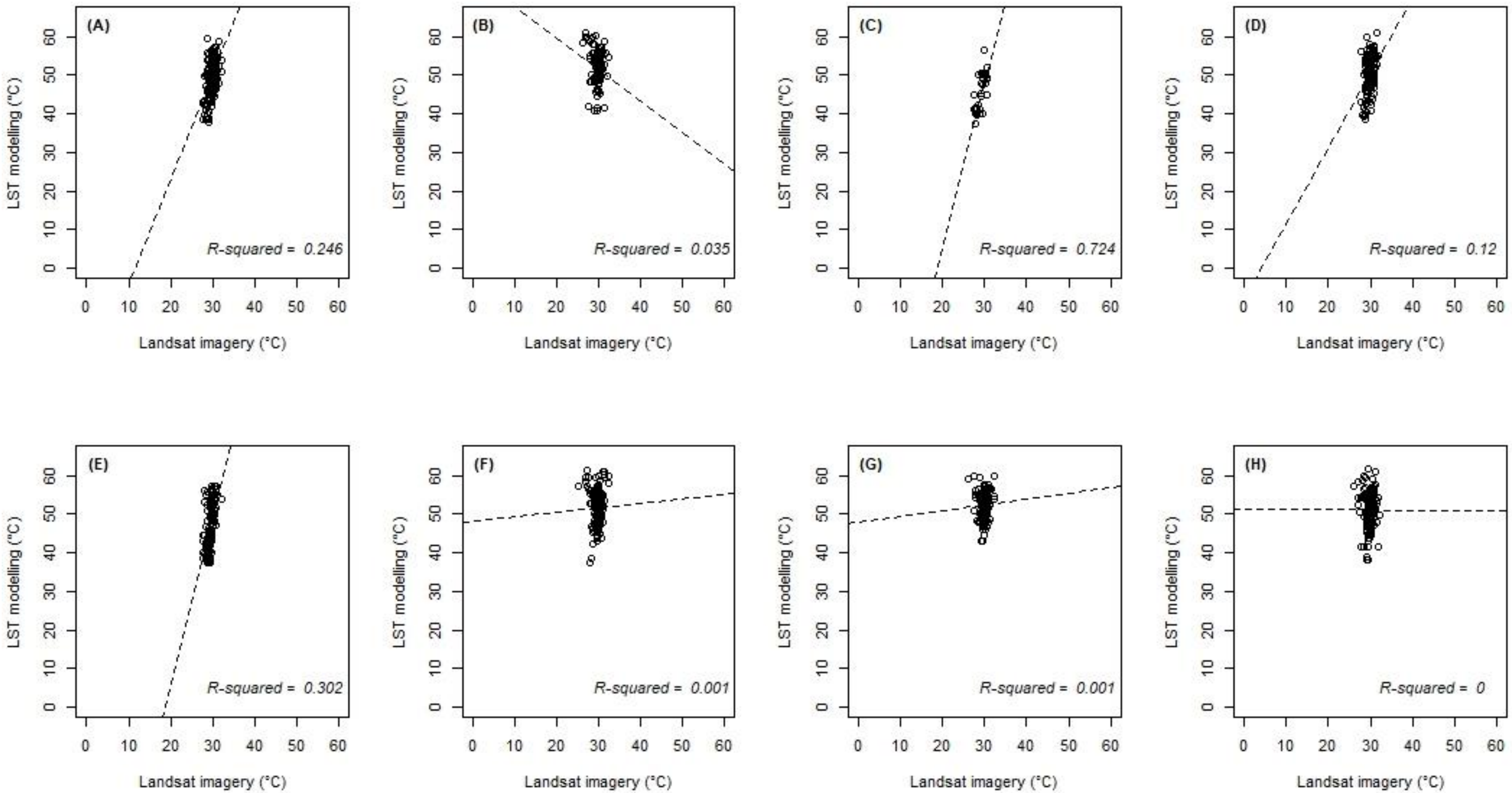

Figure 20: Correlation between Landsat thermal imagery and LST modelling for each land cover class within the Elizabeth case study area. Strength of the correlation is shown as the r-squared value within each graph. (A) Tree; (B) Water; (C) Pond/basin; (D) Dry grass; (E) Irrigated grass; (F) Roof; (G) Road; (H) Concrete.

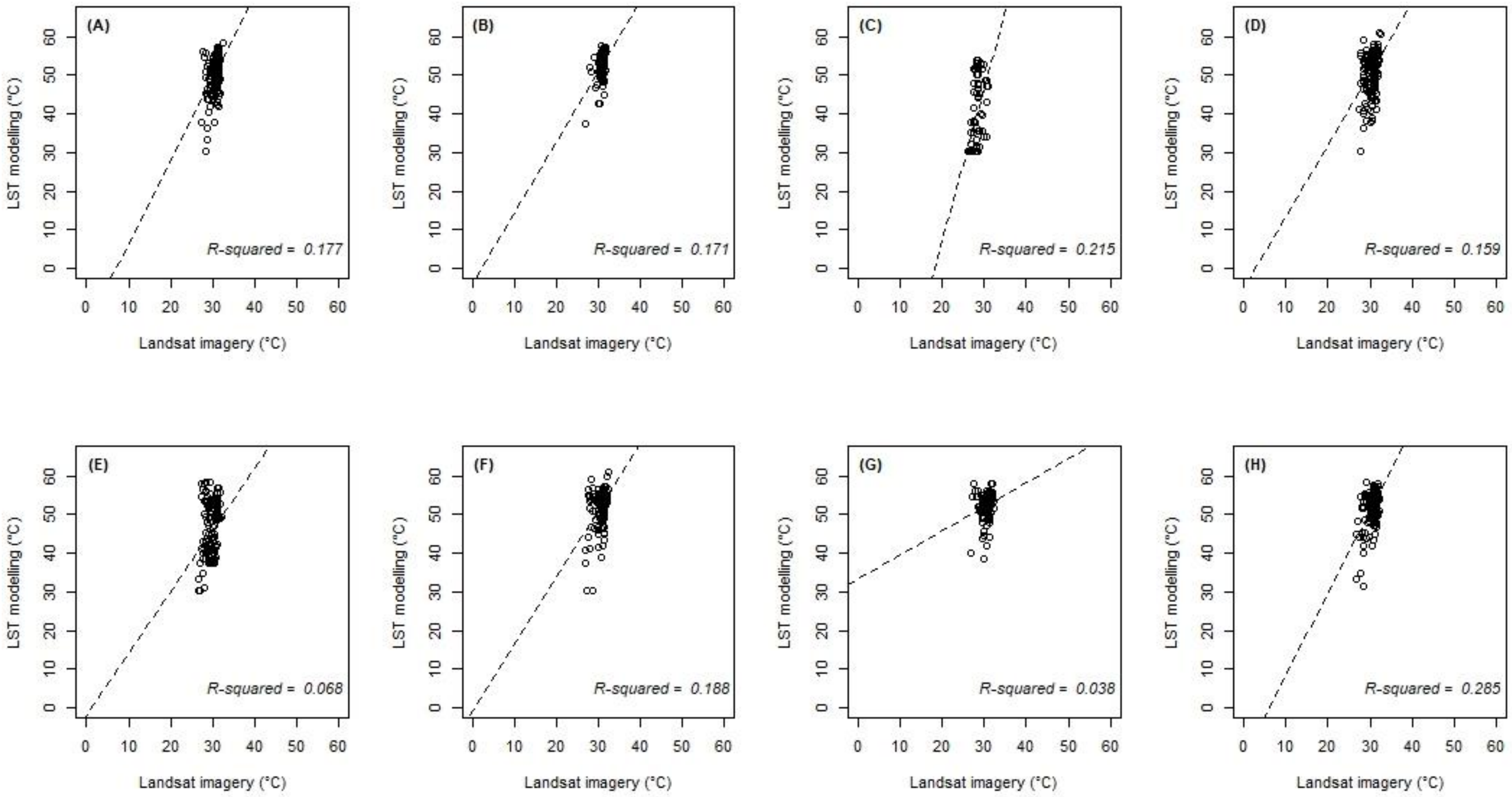

Figure 21: Correlation between Landsat thermal imagery and LST modelling for each land cover class within the Andrews Farm case study area. Strength of the correlation is shown as the r-squared value within each graph. (A) Tree; (B) Water; (C) Pond/basin; (D) Dry grass; (E) Irrigated grass; (F) Roof; (G) Road; (H) Concrete.